

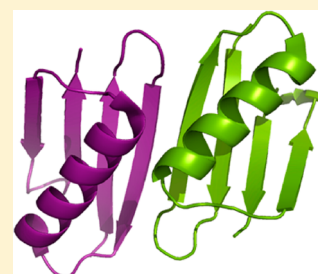
A Kinetic Approach to Determining the Conformational Stability of a Protein That Dimerizes after Folding

Stephanie Hoffmann-Thoms and Franz-Xaver Schmid*

Laboratorium für Biochemie und Bayreuther Zentrum für Molekulare Biowissenschaften, Universität Bayreuth, D-95440 Bayreuth, Germany

Supporting Information

ABSTRACT: A strongly stabilized form of the $\beta 1$ domain of the streptococcal protein G, termed G $\beta 1$ -M2, was previously obtained by an in vitro selection method for stabilized protein variants. It contains four substitutions, but how they contribute to the Gibbs free energy of denaturation (ΔG_D) could not be determined, because, unlike the wild-type protein, G $\beta 1$ -M2 dimerizes in a spectroscopically silent reaction. Here we determined the ΔG_D of the folded G $\beta 1$ -M2 monomer by using a kinetic approach that uncouples the folding of the monomer from dimerization. The conformational equilibration of the monomer is faster than dimer formation, and therefore, its stability constant could be determined from the ratio of the rate constants for monomer unfolding and refolding. In this approach, double-mixing experiments were essential for uncovering the unfolding kinetics of the transient G $\beta 1$ -M2 monomer and the association of the monomers after their folding. The analysis revealed that the selected substitutions stabilize the G $\beta 1$ -M2 monomer by 15 kJ mol⁻¹ in an additive fashion. The combination of single- and double-mixing kinetic experiments thus allowed us to determine the thermodynamic stability of a transient species that is inaccessible in equilibrium experiments. It can be applied for proteins in which monomer folding and oligomerization are kinetically uncoupled.



G $\beta 1$ is a 56-residue domain of the streptococcal protein G, which binds to the Fc part of immunoglobulins.^{1,2} It has served as a workhorse for asking basic questions about the principles of protein stability and the ambiguity of the sequence–structure code. For G $\beta 1$, it was shown that the secondary structure of an identical stretch of 11 residues was determined not by the sequence but by the structural context in the folded protein.³ Moreover, the predominantly β -sheet structure of G $\beta 1$ could be switched to the largely helical fold of G α (another, unrelated domain of protein G) by changing a single amino acid.⁴ G $\beta 1$ was also used in early attempts to stabilize proteins by computational design or by in vitro selection of variants from large libraries.^{5,6}

We used G $\beta 1$ to develop a three-step procedure for protein stabilization.⁷ In the first step, several libraries of G $\beta 1$ variants were created by error-prone polymerase chain reaction (PCR) and subjected to the in vitro selection method *Proside*. It links the increased protease resistance of stabilized protein variants to the infectivity of a filamentous phage.⁸ The substitutions found in this step were analyzed individually to identify the positions with the strongest effects on stability. In the second step, the corresponding codons were randomized by saturation mutagenesis to explore the full sequence space, and the resulting libraries were subjected to further rounds of *Proside*. Subsequently, the contributions to the stability of the selected residues were again analyzed individually, and in the final step, those with the strongest contributions were combined manually.

The most stable variant from this approach, termed G $\beta 1$ -M2, contains four substitutions (E15V, T16L, T18I, and N37L), leading to an increase in the midpoint of its thermal unfolding

transition from 51 to 86 °C in 1.5 M GdmCl.⁷ The increase in the stability of this hyperstable variant appeared to be significantly higher than the sum of the contributions of the individual substitutions. However, the analysis also showed that the stability of G $\beta 1$ -M2 increases with protein concentration. Analytical ultracentrifugation indicated that G $\beta 1$ -M2 forms dimers in solution, and the 0.88 Å crystal structure revealed how two monomers of G $\beta 1$ -M2 use a complementary hydrophobic surface to interact in the dimer (Figure 1).⁹

The thermodynamic stabilities of monomeric and dimeric forms of a protein cannot be compared. For a dimer, the conformational unfolding reaction of the monomer is linked with dimer dissociation, and thus, the measured stability becomes concentration-dependent. Dimer formation could not be suppressed by varying, for example, the pH, the salt concentration, or the polarity of the solvent.⁹

Here we employed a kinetic approach to separate the conformational unfolding transition of the G $\beta 1$ -M2 monomer from the monomer–dimer equilibration. The use of single- and double-mixing protocols allowed us to determine the rate constants of monomer unfolding and refolding as well as the association and dissociation rate constants of the dimer. The analysis revealed that the folding equilibrium is established before dimer formation, and therefore, the equilibrium constant and the Gibbs free energy (ΔG_D) for monomer unfolding could be determined as a function of the denaturant concentration

Received: February 3, 2012

Revised: April 10, 2012

Published: April 17, 2012



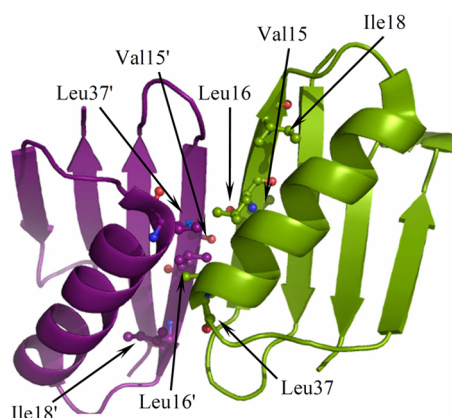


Figure 1. Crystal structure of the dimeric hyperstable variant $G\beta 1$ -M2. The monomers are assembled in a head-to-head fashion. The self-complementary interaction surface is mainly built from amino acid substitutions E15V, T16L, T18I, and N37L. These residues are shown in ball-and-stick representation. O and N atoms are colored red and blue, respectively. The figures were created using Protein Data Bank entry 3FIL⁹ and PyMOL.²³

from the ratio of the rate constants of monomer unfolding and refolding.

MATERIALS AND METHODS

Protein Purification and GdmCl-Induced Unfolding Transitions. The $G\beta 1$ gene was amplified by PCR with primers including restriction sites for *Nde*I at the N-terminus and *Bam*HI at the C-terminus. The T2Q mutation was introduced to prevent the loss of the N-terminal methionine,¹⁰ and the gene was cloned into plasmid pET11a (Novagen, Madison, WI). Introduction of the mutations, expression, and protein purification were performed as described previously^{7,9} with minor modifications.

GdmCl-induced unfolding transitions of 1 μ M wild-type $G\beta 1$ and 0.25, 1, and 10 μ M $G\beta 1$ -M2 were measured in 0.1 M sodium cacodylate-HCl (pH 7.0) and varying concentrations of GdmCl as described previously.^{7,9} The emission at 342 nm after excitation at 280 nm was measured at 25 °C in 10 mm cells with a Hitachi F-4010 fluorescence spectrophotometer. The experimental data were analyzed according to an $N \rightleftharpoons U$ two-state model¹¹ by assuming a linear dependence of the fluorescence emission on the concentration of GdmCl.

Kinetic Single-Mixing Folding Experiments. The kinetics of GdmCl-induced unfolding and refolding were measured in 0.1 M sodium cacodylate-HCl (pH 7.0) at 25 °C with final protein concentrations of 0.25 and 1.0 μ M $G\beta 1$ -M2 and 1.0 μ M wild-type $G\beta 1$ or $G\beta 1$ -M2 L37N. In all cases, native or denatured protein was diluted 11-fold to various final GdmCl concentrations. Fast unfolding and refolding kinetics were measured after stopped-flow mixing in a DX.17MV spectrometer from Applied Photophysics (Leatherhead, U.K.). After excitation at 280 nm (10 nm bandwidth), the reactions were monitored by the change in fluorescence above 340 nm in an observation chamber with a 2 mm path length. To absorb scattered light from the excitation beam, a 5 mm cell filled with acetone was placed between the observation chamber and the photomultiplier. The kinetics were measured at least eight times under identical conditions and averaged to improve the signal-to-noise ratio. The obtained chevrons of wild-type $G\beta 1$ and $G\beta 1$ -M2 L37N were analyzed according to the two-state

model¹² to calculate the microscopic rate constants of unfolding and refolding.

The unfolding reactions of 0.25 and 1.0 μ M native $G\beta 1$ -M2 and the corresponding concentration-dependent slow refolding phase were measured after manual mixing at 342 nm after excitation at 280 nm using a Hitachi F-4010 fluorescence spectrophotometer (bandwidths of 5 and 10 nm). Initially, mono- or biexponential functions were fit to the curves. Afterward, the concentration-dependent kinetic curves obtained in the folding transition region were reanalyzed as described to calculate the association and dissociation rate constants.

Kinetic Double-Mixing Experiments. To measure the unfolding branch of the chevron of the monomeric species of $G\beta 1$ -M2, fast unfolding kinetics were monitored after a short refolding pulse in a stopped-flow double-mixing experiment. In the first step, denatured protein was diluted 11-fold in 4.8 M GdmCl for 1.5 s to induce refolding of the monomer. Its unfolding kinetics was measured after a further 6-fold dilution to unfolding conditions (0.25 or 1.0 μ M $G\beta 1$ -M2 in 5.5–7.6 M GdmCl) by following the change in fluorescence above 340 nm (excitation at 280 nm). By a linear two-state analysis of the resulting chevron, the microscopic rate constants of unfolding and refolding, the equilibrium constant K_{NU} , ΔG_D , and the kinetic m values were derived.

The slow dimerization after monomer folding was followed in stopped-flow interrupted refolding experiments. Denatured $G\beta 1$ -M2 (11 μ M in 7.4 M GdmCl) was diluted 11-fold to folding conditions of 2.0, 3.0, or 3.5 M GdmCl to initiate refolding. After different delay times, unfolding was induced by a further 6-fold dilution to 7.0 M GdmCl. The fast unfolding reaction of the folded monomeric intermediate was monitored by the change in fluorescence above 340 nm after excitation at 280 nm, and monoexponential curves were fit to the data. The experiment at 3.0 M GdmCl was also performed at a 6-fold higher concentration, starting with 66 μ M unfolded protein. The resulting amplitudes of fast unfolding were plotted as a function of refolding time and analyzed on the basis of the model shown in eq 1.

Kinetic and Thermodynamic Analysis of Folding and Dimer Formation. The scheme in eq 1 was used to analyze the kinetics of folding and dimerization and to determine the corresponding equilibrium constants. U and N are the unfolded and the folded forms of the $G\beta 1$ monomer, respectively, and N_2 is the folded dimer.



The folding kinetics in Figures 4 and 5 in combination with the double-mixing experiments indicated that the unfolding and refolding of the $G\beta 1$ monomer are much faster than dimer formation and dissociation. Therefore, the kinetic chevron for monomer unfolding and refolding was analyzed separately on the basis of a linear two-state model,¹² yielding k_{UN} and k_{NU} as a function of GdmCl concentration.

Association and dissociation are silent reactions and could thus be measured only in double-mixing experiments or in the region of the unfolding transition, where the coupling between folding and dimer formation led to a shift of the folding equilibrium of the monomer and thus to a change in fluorescence during dimerization. To analyze the coupled folding and binding reaction in eq 1, we employed numerical

integration of the differential equations that describe the changes in the concentrations of U, N, and N₂ (eqs 2–4).

$$d[U]/dt = -k_{UN}[U] + k_{NU}[N] \quad (2)$$

$$d[N]/dt = k_{UN}[U] - k_{NU}[N] - 2k_{on}[N]^2 + 2k_{off}[N_2] \quad (3)$$

$$d[N_2]/dt = k_{on}[N]^2 - k_{off}[N_2] \quad (4)$$

For the analysis of the experimental data, a nonlinear least-squares fit based on the model described in eqs 1–4 was performed using Dynafit.¹³ To reduce the number of parameters in the fitting procedure, we fixed the microscopic rate constants of unfolding and refolding of the monomer, k_{NU} and k_{UN} , respectively, to the values obtained from the kinetic analysis of its chevron.

From the analysis of the observed kinetics in the transition region (4–6 M GdmCl), the rate constants of association (k_{on}) and dissociation (k_{off}) were determined and, from their ratio, the dissociation constant of the dimer (K_D^{kin}) at the corresponding denaturant concentration. At 2.0, 3.0, and 3.5 M GdmCl, association was quasi irreversible, and therefore, the calculated values for k_{off} were unreliable and not used for calculating K_D^{kin} values.

The K_D of the dimer was also calculated from the measured equilibrium transitions. Folded monomeric and dimeric species show the same fluorescence, and therefore, the apparent equilibrium constant of denaturation (K_{app}) is given by the ratio of the concentrations of the unfolded and folded molecules (eq 5).

$$K_{app} = \frac{[U]}{[N] + 2[N_2]} \quad (5)$$

The equilibrium constants for monomer unfolding (K_U) and dimer dissociation (K_D) are defined by eqs 6 and 7.

$$K_U = \frac{[U]}{[N]} \quad (6)$$

$$K_D = \frac{[N]^2}{[N_2]} \quad (7)$$

The combination of eqs 5–7 results in an expression that correlates the three equilibrium constants with the concentration of the folded monomer (eq 8).

$$\frac{[N]}{K_D} = \frac{1}{2} \left(\frac{K_U}{K_{app}} - 1 \right) = a \quad (8)$$

In the following, we designate the expression $[N]/K_D$ in eq 8 as a . The total protein concentration $[N]_0$ is given by the sum of the concentrations of the different species (eq 9)

$$[N]_0 = [N] + [U] + 2[N_2] \quad (9)$$

and the combination of eqs 6–9 gives eq 10

$$K_D = \frac{[N]_0}{a + aK_U + 2a^2} \quad (10)$$

Equation 10 relates the K_D value of dimerization with the equilibrium constant of unfolding of the monomer (K_U) and the apparent equilibrium constant for overall unfolding (K_{app}). The K_{app} value was calculated as a function of GdmCl concentration from the two-state analysis of the transition of

1 μ M G β 1-M2 in Figure 2. The equilibrium constant of unfolding K_U at different GdmCl concentrations was calculated

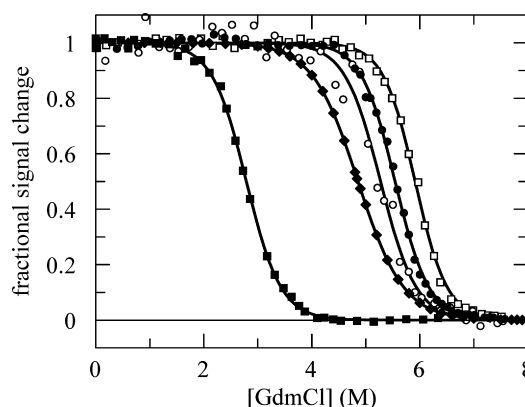


Figure 2. GdmCl-induced unfolding transitions of 1 μ M wild-type G β 1 (■) and 0.25 (○), 1 (●), and 10 μ M G β 1-M2 (□). The transitions were measured in 0.1 M sodium cacodylate-HCl (pH 7.0) at 25 °C by following the protein fluorescence at 342 nm after excitation at 280 nm. The fractional signal changes (—) were obtained after a two-state analysis of the data. The corresponding parameters are listed in Table 1. The data of the G β 1-M2 monomer transition (◆) were calculated from the ratio of the rate constants of the fast unfolding and refolding reactions of 1 μ M G β 1-M2 as a function of GdmCl concentration (Table 2).

from the microscopic rate constants of unfolding and refolding of the monomer, k_{NU} and k_{UN} , respectively, as derived from the chevron analysis.

Table 1. Stability Data for Wild-Type G β 1 and Variant G β 1-M2^a

	[protein] (μ M)	[GdmCl] _M (M)	m (kJ mol ⁻¹ M ⁻¹)	$\Delta G_D^{25\text{ °C}}$ (kJ mol ⁻¹)
wild-type G β 1	1	2.79	7.7	21.6
G β 1-M2	0.25	5.27	7.5	39.6
	1	5.54	7.9	44.0
	10	5.92	8.4	49.5

^aApparent stability parameters derived for the GdmCl-induced unfolding transitions of wild-type G β 1 and G β 1-M2 at different protein concentrations, assuming that the transitions are monomolecular two-state processes. This is an oversimplification for G β 1-M2. [GdmCl]_M is the concentration of GdmCl at the midpoint of the transition, and m is the cooperativity parameter [$m = (\partial \Delta G_D) / (\partial [\text{GdmCl}])$], calculated under the assumption of a monomolecular two-state unfolding reaction. Data were measured and analyzed as described in the legend of Figure 2.

RESULTS

Stability and Folding Kinetics of G β 1-M2. The apparent stability of G β 1-M2 increases with concentration in both thermal⁹ and denaturant-induced equilibrium unfolding transitions (Figure 2). At 1 μ M protein, the transition midpoint of G β 1-M2 is increased by 2.75 M GdmCl relative to that of the wild-type protein, which confirms that the E15V, T16L, T18I, and N37L substitutions are strongly stabilizing. However, an increase in G β 1-M2 concentration from 0.25 to 10 μ M also led to a shift of the transition midpoint to higher values (from 5.27 to 5.92 M GdmCl).

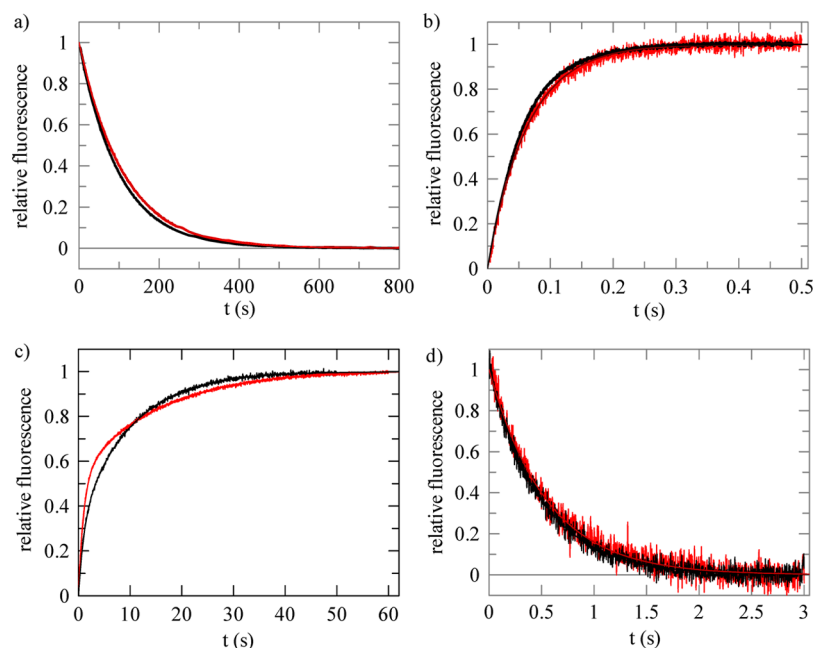


Figure 3. Normalized refolding and unfolding kinetics of 0.25 (red) and 1 μ M G β 1-M2 (black) after 11-fold dilution. (a) Unfolding of native G β 1-M2 in 7.0 M GdmCl after manual mixing (excitation at 280 nm, emission at 342 nm). The fit to the data gives time constants (τ) of 109 and 100 s at 0.25 and 1.0 μ M, respectively. (b) Monoexponential refolding kinetics at 3.0 M GdmCl starting with denatured protein in 7.4 M GdmCl (τ = 0.063 and 0.057 s at 0.25 and 1.0 μ M, respectively). (c) Refolding kinetics of denatured G β 1-M2 at 5.1 M GdmCl. Biexponential fits to the data gave a τ_1 of 1.04 s and a τ_2 of 15.31 s at 0.25 μ M G β 1-M2 and a τ_1 of 1.07 s and a τ_2 of 9.96 s at 1.0 μ M G β 1-M2. (d) Unfolding kinetics after stopped-flow double mixing. Unfolded G β 1-M2 (in 7.4 M GdmCl) was refolded in 4.8 M GdmCl for 1.5 s. Then, it was again unfolded in 7.0 M GdmCl. The resulting unfolding reactions showed τ values of 0.54 s at 0.25 μ M G β 1-M2 and 0.50 s at 1.0 μ M G β 1-M2. The reactions shown in panels b–d were followed by the change in fluorescence above 340 nm (excitation at 280 nm) after stopped-flow mixing. The solid lines represent curve fits to the data. All measurements were performed in 0.1 M sodium cacodylate-HCl (pH 7.0) at 25 $^{\circ}$ C.

The transitions in Figure 2 indicate that ≥ 7 M GdmCl is necessary to completely unfold G β 1-M2. The normalized unfolding kinetics of 0.25 and 1 μ M G β 1-M2 measured at 7.0 M GdmCl after manual mixing (Figure 3a) show that unfolding is very slow and virtually independent of the protein concentration. Both time courses in Figure 3a are governed by time constants (τ) of ~ 100 s. Additional fast unfolding reactions in the millisecond time range could not be detected after stopped-flow mixing.

Refolding of G β 1-M2 at 3.0 M GdmCl is very rapid (τ = 60 ms) and also independent of G β 1-M2 concentration (Figure 3b). This indicates that dimerization is either not a rate-limiting step in refolding or not accompanied by a change in protein fluorescence.

Refolding of 0.25 and 1 μ M G β 1-M2 was also measured near the transition midpoint at 5.1 M GdmCl (Figure 2). In this case, different time courses were observed at the two protein concentrations (Figure 3c). The tentative fit of biexponential curves to the kinetics revealed a fast reaction, which is independent of protein concentration (τ = 1.05 s) and a slow reaction that becomes faster with an increasing concentration (τ = 15.3 s at 0.25 μ M G β 1-M2, and τ = 10.0 s at 1 μ M G β 1-M2). The relative amplitude of the slow reaction increased with protein concentration. The slow reaction thus might reflect the monomer–dimer equilibration after conformational refolding of the monomer. In this case, the fit of an exponential function to the slow kinetics is an oversimplification.

To further elucidate the potential contribution of the monomer–dimer reaction to the folding mechanism of G β 1-M2, we measured the folding and unfolding kinetics at two different concentrations of G β 1-M2 (0.25 and 1 μ M) between

2.3 and 7.4 M GdmCl. The kinetic curves were again analyzed by fitting mono- or biexponential functions to the data, and the results are shown in the form of chevron plots as usual in protein folding kinetics (Figure 4). The rate of the fast reaction is independent of protein concentration and decreases with denaturant concentration, as observed in comparative experiments with wild-type G β 1 (Figure 4), and its amplitude decreases to zero near 6 M GdmCl (Figure S1 of the Supporting Information).

Between 4 and 6 M GdmCl, the refolding kinetics of G β 1-M2 are complex (Figure 4) because a slow reaction appears. The tentative fit of an exponential function to its time course gave an apparent rate that depended on both protein and denaturant concentration. It decreases ~ 100 -fold between 4 and 6 M GdmCl and becomes slightly faster with an increasing protein concentration. It is only detectable in the region where the chevron of the fast phase has its minimum, and its amplitude shows a bell-shaped dependence on denaturant concentration (Figure S1 of the Supporting Information). Such an amplitude profile is indicative of a normally silent reaction that can be detected only when it is coupled with a shift of the folding equilibrium,¹⁴ as in the transition region of the monomer.

As shown in Figure 3a, unfolding of G β 1-M2 is slow, and therefore, it could be measured after manual mixing with a high signal-to-noise ratio. At > 6 M GdmCl, unfolding was monophasic and independent of protein concentration (Figure 4). It is, however, ~ 100 -fold slower and thus not continuous with the measured rate of refolding in the transition region, unlike in the chevron of the wild-type form of G β 1 (Figure 4), where unfolding and refolding are fast and monoexponential

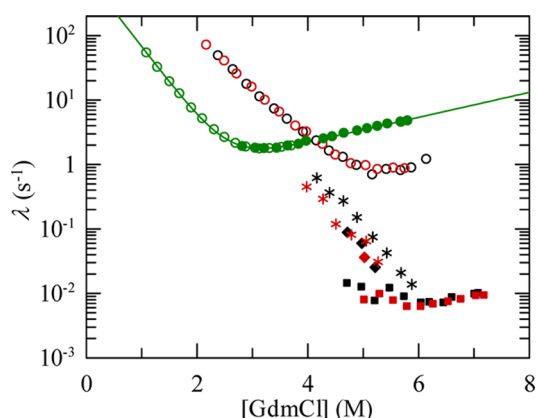


Figure 4. Apparent rate constants λ of the refolding (empty symbols) and unfolding (filled symbols) kinetics of 0.25 (red) and 1.0 μM G β 1-M2 (black) and of 1.0 μM wild-type G β 1 (green) as a function of GdmCl concentration. Refolding reactions were followed by fluorescence above 340 nm after excitation at 280 nm in single-mixing stopped-flow experiments and analyzed as the sum of exponential functions (circles and stars). The unfolding kinetics of G β 1-M2 were initiated by manual mixing and monitored at 342 nm after excitation at 280 nm. The unfolding kinetics between 4.5 and 5.2 M GdmCl were resolved into two exponential functions, the apparent rate constants of which are shown by the filled diamonds and filled squares. All measurements were performed in 0.1 M sodium cacodylate-HCl (pH 7.0) at 25 °C.

reactions at all denaturant concentrations (as observed previously under different conditions^{6,15}).

Between 4.5 and 6 M GdmCl, unfolding became complex, and a tentative decomposition into two exponential functions resulted in a faster phase that depended strongly and a slower phase that depended weakly on GdmCl concentration. The faster phase resembled the second phase of the refolding kinetics but was virtually independent of protein concentration (Figure 4).

Double-Mixing Experiments for Uncovering the Fast Unfolding Reaction of the G β 1-M2 Monomer. The very slow unfolding of G β 1-M2 and the discontinuity between the measured rates of refolding and unfolding near 6 M GdmCl (Figure 4) are unexpected. To test for the existence of additional unfolding reactions that might be masked by the slow process, we performed a stopped-flow double-mixing experiment.¹⁶ In the first step of this experiment, 1.5 or 6 μM unfolded G β 1-M2 was allowed to refold for 1.5 s at 4.8 M GdmCl. Under these conditions, the fast refolding reaction ($\tau = 1$ s) is $\sim 80\%$ complete. After this refolding pulse, the samples were unfolded by a 6-fold dilution to 7.0 M GdmCl. At both protein concentrations, the molecules that had folded during the 1.5 s refolding pulse unfolded very rapidly with a time constant of 0.5 s (Figure 3d). This unfolding reaction is 200-fold faster than the unfolding of native G β 1-M2, as observed in single-mixing experiments (Figure 3a). The product of the fast refolding reaction is thus not the native protein.

In further double-mixing experiments, the final GdmCl concentration for unfolding was varied between 5.5 and 7.4 M. The resulting rates of unfolding are independent of G β 1-M2 concentration and increase slightly with denaturant concentration. They connect with the fast refolding rates in a smooth chevron, as in the folding of wild-type G β 1 (Figure 5), and we propose that this chevron represents the folding kinetics of the G β 1-M2 monomer.

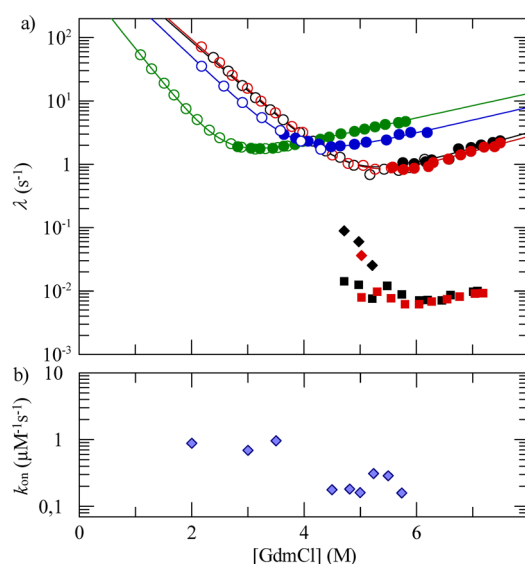


Figure 5. (a) Apparent rate constants λ of unfolding (filled symbols) and refolding (empty symbols) of 1.0 μM wild-type G β 1 (green), 1.0 μM G β 1-M2 L37N (blue), 0.25 μM G β 1-M2 (red), and 1.0 μM G β 1-M2 (black) as a function of GdmCl concentration. The folding reactions were followed by fluorescence above 340 nm after excitation at 280 nm in single-mixing stopped-flow experiments. Slow unfolding kinetics were measured after manual mixing at 342 nm after excitation at 280 nm. These data were taken from Figure 4. The rates of fast unfolding of G β 1-M2 (filled red and black circles) were obtained after stopped-flow double mixing. Denatured protein was refolded in 4.8 M GdmCl for 1.5 s and then again unfolded at the indicated GdmCl concentrations. The solid lines represent fits to the data based on a two-state model. The corresponding parameters are listed in Table 2. (b) Rate constants of association calculated from the biphasic refolding kinetics of 1.0 μM G β 1-M2 between 4 and 6 M GdmCl and from the double-mixing experiments at 2.0–3.5 M GdmCl (Figure 6 and Figure S2 of the Supporting Information) based on the kinetic model described in eq 1 in Materials and Methods. All measurements were performed in 0.1 M sodium cacodylate-HCl (pH 7.0) at 25 °C.

Double-Mixing Experiments for Uncovering the Silent Association of G β 1-M2 after Monomer Folding.

The product of the fast refolding reaction unfolds much faster than the native dimeric protein, most likely because it is still a monomer. It accumulates transiently, because the subsequent dimerization is slow. The transient monomer presumably shows nativelylike fluorescence, and therefore, dimerization is a silent reaction. To examine this, we used stopped-flow double-mixing experiments again, now to follow the time course of the fast unfolding, possibly monomeric species during refolding. Denatured G β 1-M2 (1 μM) was allowed to start refolding at 3.0 M GdmCl. At this GdmCl concentration, fluorescence-monitored refolding of G β 1-M2 is a fast monoexponential reaction with a time constant of 100 ms (Figure 4). Then, after increasing time intervals, refolding was interrupted and the sample was transferred to 7.0 M GdmCl to monitor the fast unfolding reaction. The amplitude of this reaction is a measure for the relative amount of the transient, presumably monomeric, molecules that unfold rapidly.

The time course of these fast-unfolding molecules is shown in Figure 6a. They formed almost within the dead time of stopped-flow double mixing, reached a maximum after being folded for approximately 250 ms, and then decayed in a reaction that required ~ 15 s to reach completion. This decay reaction was faster at a 6-fold higher concentration (6 μM) in

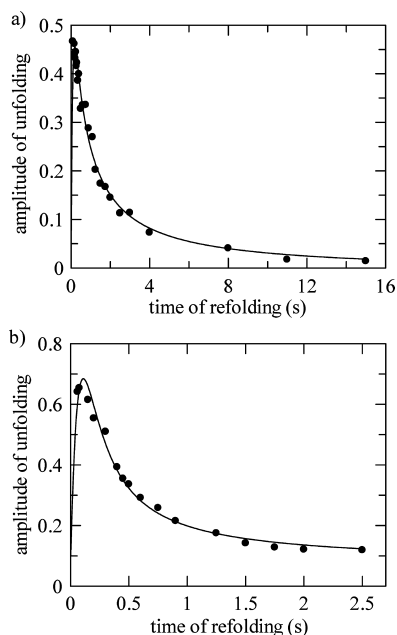


Figure 6. Time course of the population of the fast unfolding monomeric form of Gβ1-M2 during refolding of Gβ1-M2 at 3.0 M GdmCl. Refolding was initiated by an 11-fold dilution of (a) 11 and (b) 66 μM denatured Gβ1-M2 in 3.0 M GdmCl. After the indicated times of refolding, samples were transferred to unfolding conditions of 7.0 M GdmCl by a further 6-fold dilution. The amplitudes of the corresponding fast unfolding reactions are a measure for the amount of folded monomers present at the time of sampling. The solid lines represent fits obtained from an analysis of the data based on the kinetic model in eq 1 and as described in Materials and Methods. It resulted in association rates (k_{on}) of 0.69 ± 0.09 and $0.69 \pm 0.05 \mu\text{M}^{-1} \text{s}^{-1}$ at 1.0 and 6.0 μM Gβ1-M2, respectively. The kinetics were followed by fluorescence above 340 nm after excitation at 280 nm in 0.1 M sodium cacodylate-HCl (pH 7.0) at 25 °C.

the refolding step (Figure 6b), suggesting that it reflects indeed the dimerization of folded Gβ1-M2 monomers. Because it is not accompanied by a detectable change in protein fluorescence, it could not be monitored in the single-mixing experiments. The time courses shown in Figure 6 were analyzed on the basis of the kinetic scheme in eq 1 in which the folding of the monomer is followed by dimer formation. The coupled folding and binding reaction, as shown in eq 1, was analyzed by using the differential equations that describe the changes in the concentrations of U, N, and N₂ (eqs 2–4) and numerical integration. The relative fluorescence values of the unfolded and native protein, as obtained in the equilibrium unfolding

experiments, were assigned to species U and N, respectively. The monomer within the dimer (N₂) was assumed to show the same fluorescence as N. In the calculations, the rate constants of unfolding and refolding of the monomer were taken from its folding chevron (Figure 4). The analysis gave identical association rate constants of $0.69 \pm 0.09 \mu\text{M}^{-1} \text{s}^{-1}$.

Double-mixing experiments as depicted in Figure 6 were also performed at 2.0 and 3.5 M GdmCl. The corresponding time courses of the formation and decay of the monomeric intermediate are shown in Figure S2 of the Supporting Information. The analysis gave second-order rate constants for dimer formation of $0.88 \pm 0.15 \mu\text{M}^{-1} \text{s}^{-1}$ at 2.0 M GdmCl and $0.96 \pm 0.09 \mu\text{M}^{-1} \text{s}^{-1}$ at 3.5 M GdmCl, suggesting that the association of the folded Gβ1-M2 monomers is almost independent of denaturant concentration.

Between 4 and 6 M GdmCl, fluorescence-detected refolding shows a complex time course. Folding of the monomer is not complete under these conditions, and the subsequent dimerization of the folded monomer shifts the $U \rightleftharpoons N$ folding equilibrium further toward N. As a consequence, the association reaction is accompanied by a fluorescence change. The complex folding kinetics observed between 4 and 6 M GdmCl had initially been represented in the same fashion as the corresponding reactions of wild-type Gβ1 as the sum of exponential functions (Figure 4). With the knowledge that conformational folding of Gβ1-M2 is coupled with a silent dimerization, the kinetic curves obtained at 1 μM Gβ1-M2 between 4.8 and 5.8 M GdmCl were now analyzed accordingly as the sum of a fast monomolecular folding reaction and a slow bimolecular association, based on the mechanism in eq 1. In this analysis, the rate constants of unfolding and refolding of the monomer were fixed to the values obtained from the analysis of its folding chevron (Figure 5a). The rate constants of association and dissociation are listed in Table 3. The association rate constants depended weakly on GdmCl concentration (Figure 5b), and they also agreed well with the association rate constants that were derived from the double-mixing experiments at 2.0–3.5 M GdmCl. The dimerization of the Gβ1-M2 monomers is thus significantly slower than monomer folding at all GdmCl concentrations. Outside the transition region, it is silent in single-mixing experiments, because monomer folding goes to completion, and the subsequent association is not accompanied by further changes in protein fluorescence.

Stability Curve of Monomeric Gβ1-M2. In combination, the single- and double-mixing experiments demonstrate that the transient monomeric form of Gβ1-M2 is folded, and that its fast unfolding and refolding are kinetically isolated from dimer

Table 2. Stability Data for Different Gβ1 Variants Derived from the Kinetic Analysis of the Fast Folding Reaction^a

	[protein] (μM)	k_{NU} (s ⁻¹)	m_{NU} (M ⁻¹)	k_{UN} (s ⁻¹)	m_{UN} (M ⁻¹)	[GdmCl] _M (M)	m (kJ mol ⁻¹ M ⁻¹)	ΔG_D (kJ mol ⁻¹)	$\Delta\Delta G_D$ (kJ mol ⁻¹)
wild-type Gβ1	1	0.37	0.446	875	-2.56	2.58	7.5	-6.9	0
Gβ1-M2	0.25	0.033	0.553	3495	-1.81	4.90	5.9	8.2	15.1
	1	0.032	0.576	3111	-1.79	4.86	5.9	7.9	14.8
Gβ1-M2 L37N	1	0.19	0.466	2230	-1.91	3.95	5.9	2.6	9.5

^aThe kinetic parameters were determined by a linear two-state analysis of the kinetic chevrons in Figure 5. k_{NU} and k_{UN} are the microscopic rate constants of unfolding and refolding at 0 M GdmCl, respectively, m_{NU} and m_{UN} [$m_i = (\partial \ln k_i) / (\partial [\text{GdmCl}])$] are the corresponding kinetic m values. The Gibbs free energy of denaturation (ΔG_D) was calculated at 3.5 M GdmCl from the ratio of the rate constants [$\Delta G(3.5 \text{ M GdmCl}) = -RT \ln(k_{NU}/k_{UN})$]. The cooperativity parameter m [$m = RT(m_{NU} - m_{UN})$] and the transition midpoints $[\text{GdmCl}]_M$ were derived from the kinetic data. $\Delta\Delta G_D$ is the difference in Gibbs free energy of unfolding between the variants and wild-type Gβ1 at 3.5 M GdmCl. The measurements were performed as described in the legend of Figure 5.

assembly, which is slow at all denaturant concentrations. The upper chevron in Figure 5a can thus be employed to determine the microscopic rate constants of unfolding and refolding of the monomer and, from their ratio, the equilibrium constant K_{NU} as a function of GdmCl concentration. From K_{NU} , the fraction of native protein was calculated, and the corresponding transition curve is included in Figure 2. It represents the stability transition of the folded monomeric form of G β 1-M2.

The ΔG_{D} and m values derived from the two-state analysis of the kinetic folding data for the monomer are virtually identical at 0.25 and 1.0 μM G β 1-M2 (Table 2) as expected for the folding transition of a monomeric protein. The cooperativity m value is slightly smaller for monomeric G β 1-M2 than for wild-type G β 1 (Table 2), possibly because the G β 1-M2 monomer exposes more hydrophobic surface in the folded form already (which ultimately causes dimer formation).⁹

To minimize errors that originate from long extrapolation to 0 M GdmCl, we compared the stabilities of wild-type G β 1 and the G β 1-M2 monomer at 3.5 M GdmCl, which is between the transition midpoints of the two variants. Here, monomeric G β 1-M2 shows an increase in stability of 15.1 kJ mol⁻¹ (Table 2). Previously, the contributions to stability of the four amino acid substitutions in G β 1-M2 were determined individually by thermal unfolding transitions in 1.5 M GdmCl of variants with the corresponding single substitutions.¹⁷ The sum of these four contributions amounted to 15.3 kJ mol⁻¹, which agrees surprisingly well with the stabilization derived from the kinetic analysis of the transient monomeric form of G β 1-M2, which contains all four substitutions.

The back substitution of Leu37 to the wild-type residue Asn converts G β 1-M2 to a monomer¹⁷ because it prevents the formation of the complementary hydrophobic surface that is essential for dimerization.⁹ G β 1-M2 L37N in fact shows concentration-independent monoexponential folding kinetics at all GdmCl concentrations. The corresponding chevron (Figure 5) displays virtually the same slopes as the chevron of the G β 1-M2 monomer. The analysis gave a loss of stability of 5.3 kJ mol⁻¹ relative to that of the G β 1-M2 monomer (Table 2). Again, this value is similar to the stabilization by 6.0 kJ mol⁻¹, caused by the inverse substitution (N37L) in wild-type G β 1.⁹ In summary, these comparisons indicate that the kinetic analysis of the G β 1-M2 monomer is valid and that the contributions to stability of the four substitutions are additive in G β 1-M2.

Stability of the G β 1-M2 Dimer. The folding equilibrium of the G β 1-M2 monomer and its association are coupled reactions (eq 1). The dissociation constant of the dimer (K_{D}) can therefore be determined from the apparent overall equilibrium constant K_{app} (eq 5), as obtained from the transitions in Figure 3 and from the stability constant of the monomer, K_{U} , as calculated from the folding kinetics of the monomer. The analysis was performed for 1 μM G β 1-M2 between 4.8 and 5.8 M GdmCl, conditions under which K_{app} and K_{U} could be determined with good accuracy (cf. Figure 3). A K_{D} value of $0.03 \pm 0.02 \mu\text{M}$ was obtained, and to a first approximation, this value was independent of G β 1-M2 concentration. This confirms that, in fact, G β 1-M2 forms a stable dimer and explains why the apparent stability of G β 1-M2 remains concentration-dependent below 1 μM . The dissociation constant was also calculated from the ratio of the rate constants of dimer dissociation and association ($k_{\text{off}}/k_{\text{on}}$), and these values agreed with those obtained from the equilibrium transitions within the limits of confidence (Table 3).

Table 3. Dissociation Constants of the G β 1-M2 Dimer in the Unfolding Transition Region^a

[GdmCl] (M)	k_{on} ($\mu\text{M}^{-1} \text{s}^{-1}$)	k_{off} (s^{-1})	$K_{\text{D}}^{\text{kin}}$ (μM)	K_{D}^{eq} (μM)
5.74	0.16	0.007	0.05	0.05
5.50	0.29	0.005	0.02	0.05
5.24	0.24	0.003	0.01	0.04
4.99	0.12	0.001	0.01	0.03
4.81	0.18	0.002	0.01	0.02

^aThe rates of association and dissociation were determined from the analysis of the slow phase of the refolding kinetics of 1 μM G β 1-M2 after manual mixing using the model described in eq 1 and DynaFit.¹³ $K_{\text{D}}^{\text{kin}}$ was calculated from the ratio of the rate constants ($K_{\text{D}}^{\text{kin}} = k_{\text{off}}/k_{\text{on}}$). K_{D}^{eq} was calculated from the measured overall equilibrium constant K_{app} and the stability constant of the monomer, K_{U} , in Figure 2 and by using eq 8.

DISCUSSION

G β 1-M2 resulted from an in vitro selection for stabilized protein variants. It is a dimer in solution, and therefore, the folding transition of the monomers is coupled with dimerization. As a consequence, in terms of conformational stability (ΔG_{D}), G β 1-M2 could not be compared to the wild-type form or to other stabilized variants of G β 1, which all are monomeric. Here we determined the ΔG_{D} of the G β 1-M2 monomer by using a kinetic approach that uncoupled monomer folding from dimerization. This was feasible because unfolding and refolding of the monomer were faster than dimer formation and dissociation over the entire range of denaturant concentrations. The lifetime of the folded monomer was long enough to establish its folding equilibrium, and the stability constant could be determined from the ratio of the rate constants of refolding and unfolding. For this approach to be successful, it was essential to combine conventional single-mixing folding experiments with double-mixing experiments, in which a brief refolding pulse was followed by unfolding.¹⁶ Thus, the unfolding of the G β 1-M2 monomer and the association of the folded monomers could be uncovered. Both reactions are silent in single-mixing unfolding or refolding experiments.

The four selected substitutions in G β 1-M2 are in fact strongly stabilizing. Together, they increased the stability of the G β 1-M2 monomer by 15 kJ mol⁻¹. This value is smaller than the value of 27.2 kJ mol⁻¹, which was calculated originally under the erroneous assumption that G β 1-M2 is a monomer.⁷ It is, however, higher than the extent of stabilization reached for G β 1 in previous in vitro selection experiments.^{5,6,17,18}

The individual contributions of the four substitutions to the stability of the G β 1-M2 monomer are additive. Previously, they were measured for four variants with single substitutions, and their sum (15.3 kJ mol⁻¹)^{7,9} is almost identical with the stabilization by 15 kJ mol⁻¹ observed for the G β 1-M2 monomer with all four substitutions. Such a good agreement is remarkable, with regard to the fact that the stabilities of the individual variants were calculated from thermal unfolding transitions at 70 °C in 1.5 M GdmCl, and the stability of the G β 1-M2 monomer was calculated at 25 °C in the presence of 3.5 M GdmCl.

Dimer or oligomer formation provides a general means to increase the stability of proteins, in particular at high temperatures, and accordingly, enzymes from hyperthermophilic organisms often exist in larger oligomeric complexes than their homologues from mesophilic organisms.^{19–21} In principle, it is impossible to compare the thermodynamic stabilities of

monomeric and oligomeric forms of a protein, because the stability of the oligomer depends on protein concentration, and the standard state (1 M reactants and product) is physically unreasonable for macromolecules. To turn differences in stability of related monomeric and oligomeric species into numbers, usually, qualitative or semiquantitative measures of protein stability are used, such as the rate of irreversible thermal inactivation,¹⁹ CD-monitored thermal unfolding,²² or calorimetry,²¹ always at identical monomer concentrations. By these measures, the oligomeric forms were found to be more “stable” in all cases. Differences in ΔG_D can, however, not be determined by these approaches. Furthermore, it is not possible to dissect the impact of sequence differences on the stability of the monomers and the strength of their interactions in the oligomeric form of the protein. This information can be obtained for proteins for which the folding equilibrium of the monomers is established faster than their association by combining equilibrium measurements with single- and double-mixing kinetic folding experiments, as we showed here for G β 1-M2.

■ ASSOCIATED CONTENT

● Supporting Information

Two figures with supporting data on the folding kinetics. This material is available free of charge via the Internet at <http://pubs.acs.org>.

■ AUTHOR INFORMATION

Corresponding Author

*Biochemie, Universität Bayreuth, D-95440 Bayreuth, Germany. Telephone: ++49 921 553660. Fax: ++49 921 553661. E-mail: fx.schmid@uni-bayreuth.de.

Funding

Supported by the Deutsche Forschungsgemeinschaft.

Notes

The authors declare no competing financial interest.

■ ACKNOWLEDGMENTS

We thank Jochen Reinstein and the members of our groups for many discussions about this work.

■ ABBREVIATIONS

G β 1, β 1 domain of streptococcal protein G; G β 1-M2, hyperstable variant of G β 1 containing the E15V, T16L, T18I, and N37L substitutions; ΔG_D , Gibbs free energy of denaturation; [GdmCl]_M, concentration of GdmCl at the midpoint of the transition; m , cooperativity parameter [$m = RT(m_{NU} - m_{UN})$]; GdmCl, guanidinium chloride; λ , apparent rate constant of a reaction; τ , time constant ($\tau = \lambda^{-1}$); k_{NU} and k_{UN} , microscopic rate constants of unfolding and refolding, respectively; m_{NU} and m_{UN} , kinetic m values for unfolding and refolding, respectively; K_{NU} , equilibrium constant of unfolding; k_{on} and k_{off} , association and dissociation rate constants, respectively; K_D , dissociation constant of the dimer; K_{app} , apparent overall equilibrium constant.

■ REFERENCES

(1) Gronenborn, A. M., Filpula, D. R., Essig, N. Z., Achari, A., Whitlow, M., Wingfield, P. T., and Clore, G. M. (1991) A novel, highly stable fold of the immunoglobulin binding domain of streptococcal protein G. *Science* 253, 657–661.

(2) Gallagher, T., Alexander, P., Bryan, P., and Gilliland, G. L. (1994) Two crystal structures of the B1 immunoglobulin-binding domain of streptococcal protein G and comparison with NMR. *Biochemistry* 33, 4721–4729.

(3) Minor, D. L., and Kim, P. S. (1994) Context is a major determinant of β -sheet propensity. *Nature* 371, 264–267.

(4) He, Y., Chen, Y., Alexander, P., Bryan, P. N., and Orban, J. (2008) NMR structures of two designed proteins with high sequence identity but different fold and function. *Proc. Natl. Acad. Sci. U.S.A.* 105, 14412–14417.

(5) Malakauskas, S. M., and Mayo, S. L. (1998) Design, structure and stability of a hyperthermophilic protein variant. *Nat. Struct. Biol.* 5, 470–475.

(6) Wunderlich, M., Martin, A., Staab, C. A., and Schmid, F. X. (2005) Evolutionary protein stabilization in comparison with computational design. *J. Mol. Biol.* 351, 1160–1168.

(7) Wunderlich, M., and Schmid, F. X. (2006) In vitro evolution of a hyperstable G β 1 variant. *J. Mol. Biol.* 363, 545–557.

(8) Sieber, V., Plückthun, A., and Schmid, F. X. (1998) Selecting proteins with improved stability by a phage-based method. *Nat. Biotechnol.* 16, 955–960.

(9) Thoms, S., Max, K. E. A., Wunderlich, M., Jacso, T., Lilie, H., Reif, B., Heinemann, U., and Schmid, F. X. (2009) Dimer Formation of a Stabilized G β 1 Variant: A Structural and Energetic Analysis. *J. Mol. Biol.* 391, 918–932.

(10) Smith, C. K., Withka, J. M., and Regan, L. (1994) A thermodynamic scale for the β -sheet forming tendencies of the amino acids. *Biochemistry* 33, 5510–5517.

(11) Santoro, M. M., and Bolen, D. W. (1988) Unfolding free energy changes determined by the linear extrapolation method. 1. Unfolding of phenylmethanesulfonyl α -chymotrypsin using different denaturants. *Biochemistry* 27, 8063–8068.

(12) Schindler, T., and Schmid, F. X. (1996) Thermodynamic properties of an extremely rapid protein folding reaction. *Biochemistry* 35, 16833–16842.

(13) Kuzmic, P. (2009) DynaFit: A software package for enzymology. *Methods Enzymol.* 467, 247–280.

(14) Kiefhaber, T., Kohler, H. H., and Schmid, F. X. (1992) Kinetic Coupling Between Protein Folding and Prolyl Isomerization. 1. Theoretical Models. *J. Mol. Biol.* 224, 217–229.

(15) McCallister, E. L., Alm, E., and Baker, D. (2000) Critical role of β -hairpin formation in protein G folding. *Nat. Struct. Biol.* 7, 669–673.

(16) Schmid, F. X. (1983) Mechanism of folding of ribonuclease A. Slow refolding is a sequential reaction via structural intermediates. *Biochemistry* 22, 4690–4696.

(17) Wunderlich, M., Max, K. E., Roske, Y., Mueller, U., Heinemann, U., and Schmid, F. X. (2007) Optimization of the G- β 1 domain by computational design and by in vitro evolution: Structural and energetic basis of stabilization. *J. Mol. Biol.* 373, 775–784.

(18) Dahiyat, B. I., and Mayo, S. L. (1997) Probing the role of packing specificity in protein design. *Proc. Natl. Acad. Sci. U.S.A.* 94, 10172–10177.

(19) Thoma, R., Hennig, M., Sterner, R., and Kirschner, K. (2000) Structure and function of mutationally generated monomers of dimeric phosphoribosylanthranilate isomerase from *Thermotoga maritima*. *Structure* 8, 265–276.

(20) Clantin, B., Tricot, C., Lonhienne, T., Stalon, V., and Villeret, V. (2001) Probing the role of oligomerization in the high thermal stability of *Pyrococcus furiosus* ornithine carbamoyltransferase by site-specific mutants. *Eur. J. Biochem.* 268, 3937–3942.

(21) Schwab, T., Skegro, D., Mayans, O., and Sterner, R. (2008) A rationally designed monomeric variant of anthranilate phosphoribosyltransferase from *Sulfolobus solfataricus* is as active as the dimeric wild-type enzyme but less thermostable. *J. Mol. Biol.* 376, 506–516.

(22) Schliebs, W., Thanki, N., Jaenicke, R., and Wierenga, R. K. (1997) A double mutation at the tip of the dimer interface loop of triosephosphate isomerase generates active monomers with reduced stability. *Biochemistry* 36, 9655–9662.

(23) DeLano, W. L. (2003) *The PyMOL Molecular Graphics System*, DeLano Scientific LLC, San Carlos, CA.